Applied Surface Science 259 (2012) 811–815

Contents lists available at SciVerse ScienceDirect

Applied Surface Science

journal homepage: www.elsevier.com/locate/apsusc

Magnetron sputtering SiC films on nickel photonic crystals with high emissivity for high temperature applications

Zhenyu Li[a], Lili Yang[b], Dengteng Ge[a], Yanbo Ding[c], Lei Pan[a], Jiupeng Zhao[c], Yao Li[a,*]

[a] Center for Composite Materials and Structure, Harbin Institute of Technology, Harbin 150001, China
[b] School of Transportation Science and Engineering, Harbin Institute of Technology, Harbin 150090, China
[c] School of Chemical Engineering and Technology, Harbin Institute of Technology, Harbin 150001, China

ARTICLE INFO

Article history:
Received 11 April 2012
Received in revised form 9 July 2012
Accepted 23 July 2012
Available online 31 July 2012

Keywords:
Emissivity
SiC
Sputtering
Patterned structure

ABSTRACT

High emissivity coatings have been widely used in many high temperature applications. Here we report a novel structure of magnetron sputtering silicon carbide (SiC) films on Ni photonic crystals (PCs) to improve emissivity performance. It is found that SiC coatings reveal two-dimensional patterned structures due to their preferential growth on the skeleton of Ni PCs. The spectral emissivity results show periodic structures and surface-porous structured SiC can enhance the coatings' spectral emissivity because of higher rough surface, lower reflectivity and magnitude of thermal fluctuations. The method holds promising potential for preparing a series of high emissivity coatings and highly ordered metal–ceramics composites microstructures for thermophotovoltaic (TPV) radiator, pyroelectric and other photonics applications.

© 2012 Elsevier B.V. All rights reserved.

1. Introduction

High emissivity coatings are key technologies to effectively transfer the radiation for TPV or thermal protection system especially at high temperature. Many potential materials have been proposed as high emissivity coatings such as SiO_2, ZrO_2, SiC and indium tin oxide [1–4]. Among these materials, SiC has been extensively studied because of its low density, excellent chemical stability and thermal stability. It is widely accepted that approaches to enhance the emissivity involve the design of doping, surface roughness, surface texture, coating thickness, architecture, etc. [5–10]. Recently, photonic crystals (PCs) have stimulated enormous interest as promising architectures due to their manipulation electromagnetic waves' propagation [11]. They have been considered as thermal barrier coatings for high temperature applications [12]. Yeng have reported that tungsten PCs periodically in one dimension prepared by interferometric lithography and reactive ion etching can provide high emissivity for TPV applications [13]. A lot of papers were published about the fabrication or photoluminescence studies of SiC PCs [14,15]. However, lack of proper SiC precursor, poor film integrity, bad wear-resistant and low mechanical strength result in unsuitability for practical applications. Therefore, high emissivity SiC coatings with PCs structure prepared by facile methods have not been achieved.

In this paper, SiC coatings with PCs structure have been successfully prepared by template-assisted electrodeposition and magnetron sputtering methods with high thermal stability and excellent mechanical properties. Their growth mechanism and the improved thermal emissivity properties were also studied.

2. Experimental

2.1. Preparation of Ni PCs

Ni PCs possessing excellent mechanical properties were fabricated using template-assisted electrodeposition method as described in our previous paper [16]. Firstly polystyrene (PS) templates were fabricated on nickel alloy substrates using a controlled vertical drying method. Then Ni was infiltrated by electrodeposition under a constant cathode current density of 0.03 A/cm^2 for a few minutes. Finally Ni PCs were obtained after the removal of PS templates by immersion in toluene. Ni films without PCs structure were also fabricated on nickel alloy substrates by electrodeposition.

2.2. Fabrication of SiC

SiC films were achieved through RF magnetron sputtering method using a SiC target (99.9% purity). The sputtering was performed with RF power of 140 W under Ar pressure of 5 Pa. Coatings

* Corresponding author. Tel.: +86 451 86403767; fax: +86 451 86403767.
E-mail addresses: yaoli@hit.edu.cn, lizy_2006@126.com (Y. Li).

0169-4332/$ – see front matter © 2012 Elsevier B.V. All rights reserved.
http://dx.doi.org/10.1016/j.apsusc.2012.07.129

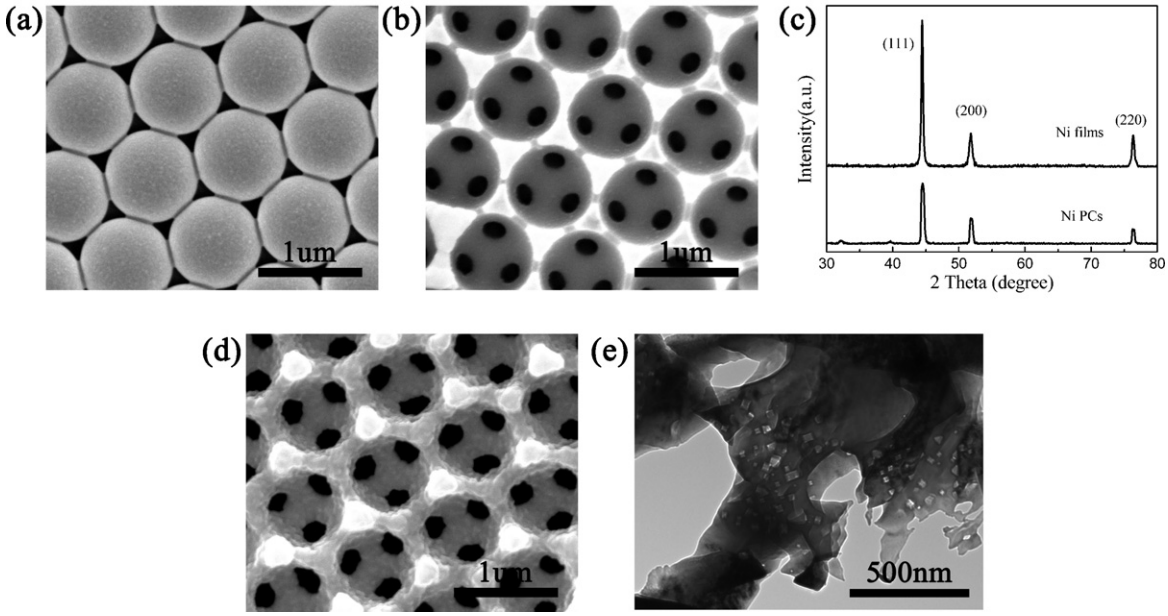

Fig. 1. SEM images of (a) PS templates; (b) Ni PCs before annealing; (c) XRD of Ni PCs and pure Ni films; (d) Ni PCs after annealing; and (e) TEM of Ni PCs after annealing.

were deposited at 500 K for 1 h, 2 h, 3 h, respectively. For comparison, other SiC coatings on Ni films were also performed. After deposition, the coatings were annealed at 1000 K with an N_2 atmosphere for 1 h to increase the crystallization process.

2.3. Testing and characterization

The surface morphologies and structural information of coatings were characterized with a Hitachi S-4800 scanning electron microscope (SEM) operating at 20 kV and transmission electron microscope (TEM Tecnai G2 F30). X-ray diffraction (XRD), energy dispersive X-ray spectroscopy (EDX) and X-ray photoelectron spectroscopy (XPS) measurements were performed to determine the elemental composition. The spectral emissivity of coatings on Ni film and Ni PCs were investigated at 600 K and 800 K, respectively using Fourier transform infrared (FTIR, JASCO-6100) spectrometer.

3. Results and discussion

3.1. Characterization of Ni PCs

Fig. 1(a) shows the SEM image of PS templates covered on nickel alloy, which reveals the PS arranged in a face-centered cubic lattice with diameters of 900 nm based on center-to-center measurements. In Fig. 1(b) a perfect ordered structure with smooth surfaces of Ni PCs appears and no obvious shrinkage occurs during the electrodeposition. Fig. 1(c) displays the XRD pattern of Ni PCs and pure Ni films before annealing. The peaks at $2\theta = 44.5^\circ$, 51.9° and 76.2° can be indexed as (1 1 1), (2 0 0) and (2 2 0) planes of Ni (JCPDF#04-0850). The crystalline grain size estimated using Debye–Scherrer formula from the width of (1 1 1) peak at half maximum is 17 nm for Ni PCs and 27 nm for Ni pure films. That indicates ordered macroporous structures in Ni PCs does not alter the nanocrystalline grain size of the deposited films and the grain growth remains priority long (1 1 1). Fig. 1(d) shows the micrograph of Ni PCs after annealing at 1000 K under N_2 atmosphere for 1 h. It is apparent that Ni particles grow slightly during the annealing process. Ni PCs do not drive obvious grain agglomeration that can result in severe structural degradation. The average grain size of 3DOM Ni after annealing is about 320 nm, obtained from Fig. 1(e), but Ni PCs retain its ordered macroporous structures. Furthermore, the nickel skeletons in the macroporous structure do not break due to diffusion, melting or mechanical stress. These indicate that Ni PCs highly suppress the agglomeration of crystalline particles and possess excellent thermal stability.

3.2. Morphology variation of Ni PCs/SiC

Fig. 2 shows the typical SEM images of SiC coatings on Ni PCs formed at different deposition time and on pure Ni films, which can reflect the deposition process of SiC coatings. Fig. 2(a) demonstrates that deposition begins with the accumulation of SiC on the surfaces of Ni skeleton. SiC preferentially grows at the surface skeleton and then penetrates to the interior of macropores. It is clear that patterned SiC structure can be obtained when the deposition time is 2 h. However, SiC is unable to fill the pores completely, which leads to a structure similar to two-dimensional gratings. With the increase of deposition time, SiC gradually penetrates into the macropores and approaches to be a dense layer, as shown in Fig. 2(c). The EDX spectroscopy shows that only Ni, C, Si, and O present in the coatings. The schematic growth process of SiC on Ni PCs is summarized in Fig. 2(e). The cross-section SEM of Ni PCs/SiC coatings prepared under the deposition time of 3 h is shown in Fig. 2(f). The thickness of Ni PCs and SiC layer is about 2.5–3 μm and 2–2.5 μm, respectively. Fig. 1(g) and (h) presents the top-viewed and cross sectional images of SiC coatings deposited on pure Ni films, respectively. Dense and uniform SiC coatings are fabricated and the thickness is around 2.5 μm. Li has reported the growth of hierarchical amorphous TiO_2 nanocolumn arrays using a PS colloidal as template, as TiO_2 only aggregating in the surface of PS and formatting of TiO_2/PS composite structure [17]. Jeong also reported the fabrication of Si nanocone/polymer solar cells by the conformal growth of PEDOT:PSS over the Si nanocones [18]. Here, it is interesting to find that the growth of SiC coatings on Ni PCs also has the duplicating phenomenon. Combining above results, the formation mechanism of hierarchical Ni PCs/SiC patterned coatings can be easily understood. The interfaces between Ni PCs and SiC layer are obscure, which is caused by the penetration of SiC into the pores

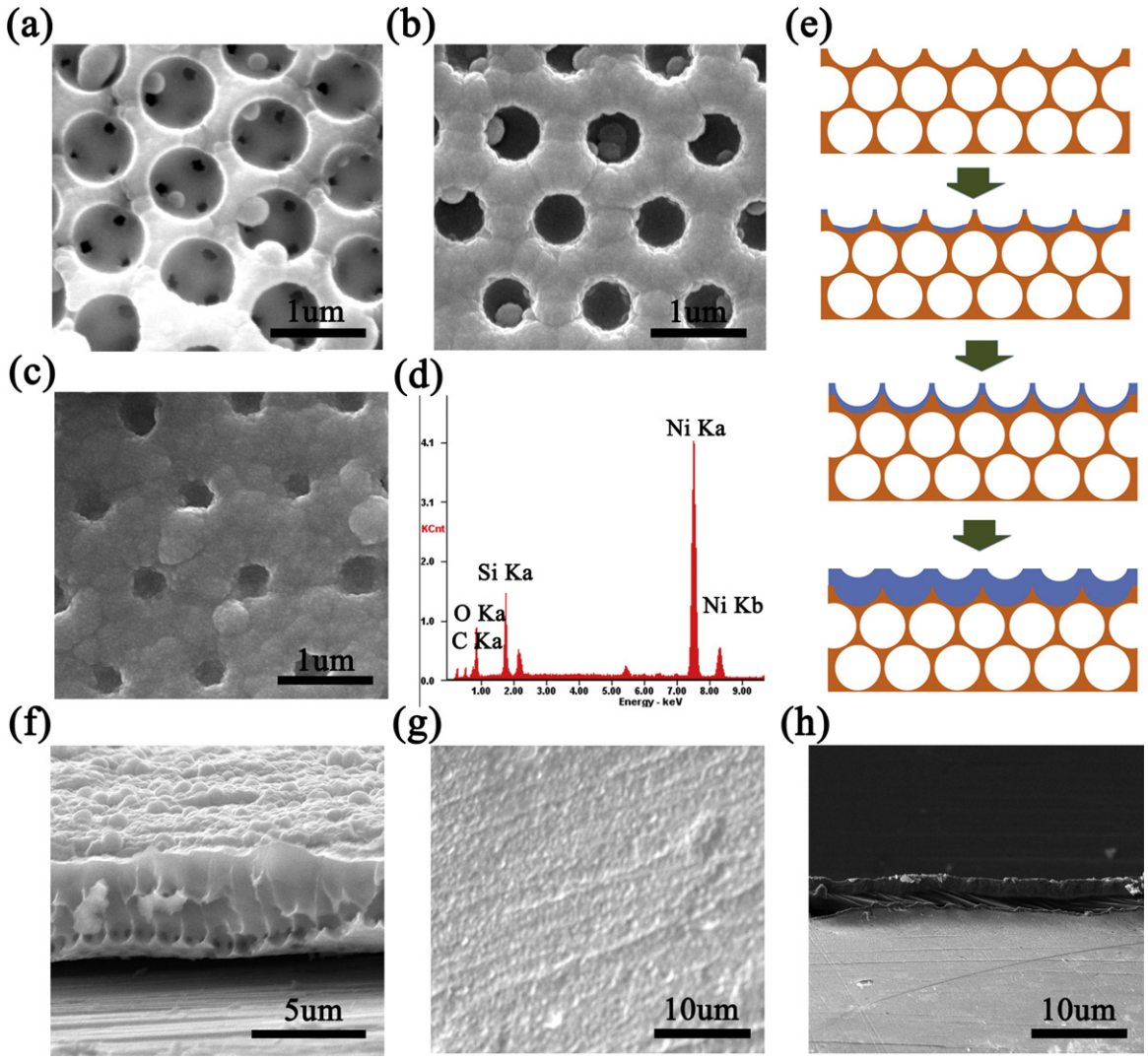

Fig. 2. SEM images of Ni PCs/SiC coatings prepared at different deposition time: (a) 1 h; (b) 2 h; (c) 3 h; and (d) the corresponding EDX; (e) the schematic illustration of formation mechanism of Ni PCs/SiC coatings; (f) cross-sectional SEM image of Ni PCs/SiC coatings; (g) and (h) are top-viewed and cross sectional images of SiC coating on pure Ni films.

of Ni PCs. These structures promise that Ni PCs/SiC coatings have excellent mechanical properties for high thermal applications as high emissivity coatings.

3.3. XRD and XPS analyses

Fig. 3(a) shows XRD spectra of SiC coatings. The features are from the Ni PCs and Ni alloy substrate. No intense diffraction peaks of crystalline SiC can be observed, indicating the formation of amorphous SiC. Fig. 3(b) and (c) shows the XPS spectra of C 1s and Si 2p of the coatings annealed at 1000 K. According to the previous reports [19], the C 1s peak can be divided into two compositions situated at 283.1 eV and 284.8 eV that are associated to the Si—C and the C—C bond, respectively. The C—C bonds come from amorphous graphite. The XPS spectra of Si 2p in Fig. 2(b) show the peaks indicating the formation of Si—O, Si—C, C—O—Si in the coatings. These XPS results demonstrate the formation of SiC.

3.4. Emissivity characterization

Fig. 4 displays the spectral emissivities of Ni PCs/SiC coatings at different temperatures and the emissivities of Ni/SiC coatings without PCs for comparison. The coatings are the samples which the deposition time is 2 h. It is found that with the increase of temperature, the emissivities of coatings are enhanced. Compared with Ni/SiC coatings, the spectral emissivity of Ni PCs/SiC patterned coatings increases at the same condition. At shorter wavelength of 4–8 μm the average emissivity increases from 0.611 to 0.642 at 600 K and from 0.624 to 0.719 at 800 K after the PCs were introduced. At longer wavelengths of 8–20 μm it increases from 0.646 to 0.667 at 600 K and from 0.707 to 0.789 at 800 K.

The emissivity increases by roughly 15% at the shorter wavelengths and 12% at the longer wavelengths. The enhancement of emissive performance is attributed to both the rough surfaces and the ordered structures. In one side, the increased surface area fraction of air-to-SiC decreases the index contrast, resulting in a slightly lower reflectivity and the emissivity of the patterned structure can increase via Kirchhoff's law of thermal radiation [13,20]. In the other side, the enhancement of emissivity may also be caused by periodic structures that can affect the coating's density of states. Excessive thermal emission can be provides by PCs due to PCs can modify not only the magnitude of thermal fluctuations but also the expectation value of thermal radiation intensity [21,22]. All these demonstrate the periodic structures and patterned surfaces play an extraordinary important role in the enhancement of emissivity performance.

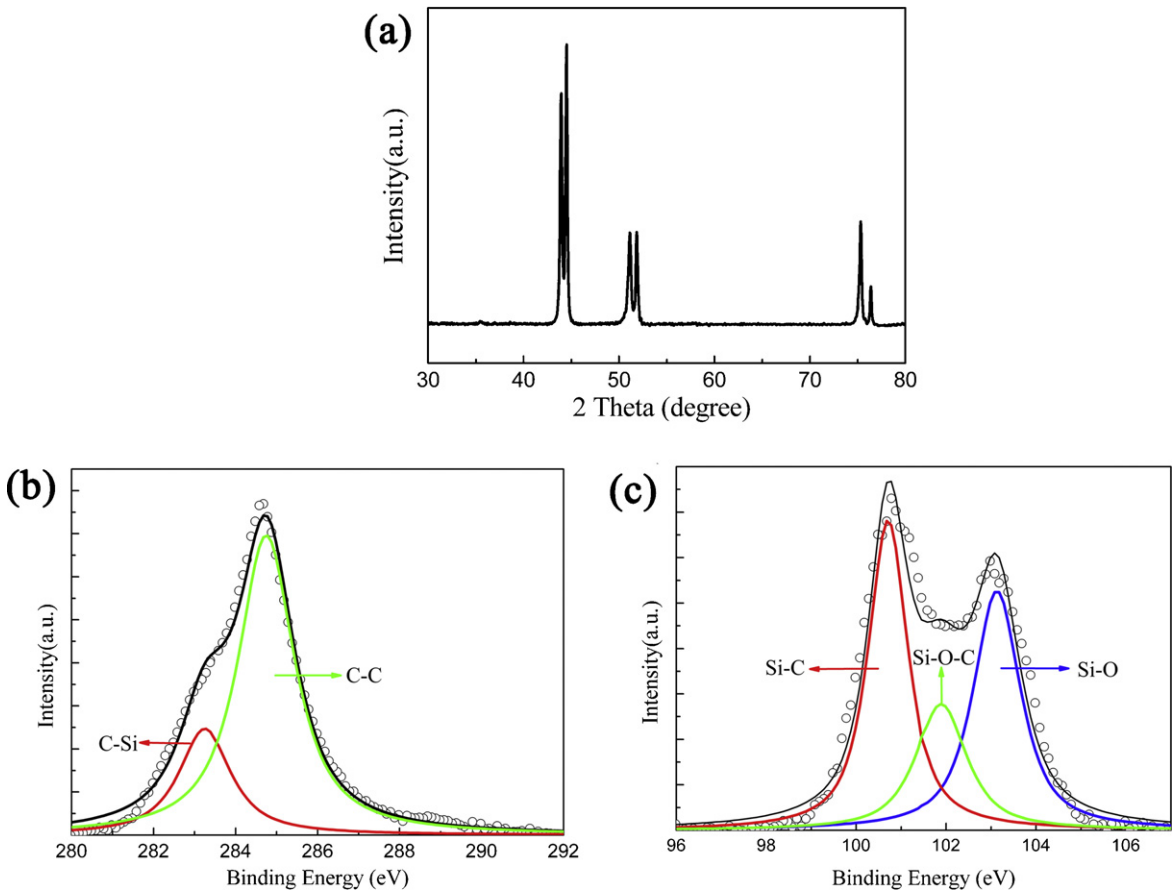

Fig. 3. XRD pattern of (a), XPS spectra of (b), C 1s and (c) Si 2p of Ni PCs/SiC coatings.

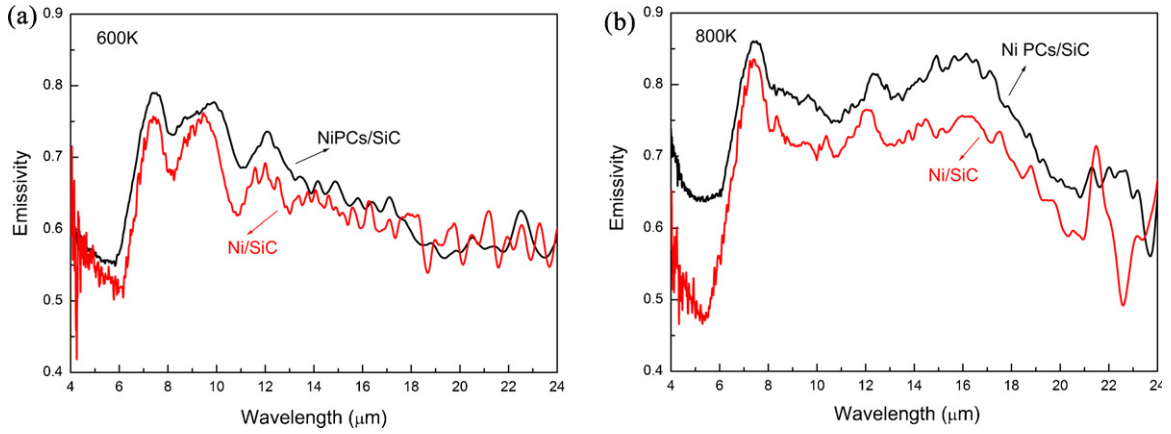

Fig. 4. Spectral emissivity of Ni/SiC and Ni PCs/SiC coatings at (a) 600 K and (b) 800 K.

4. Conclusions

In this paper, a novel structure has been fabricated to improve emissive performance by magnetron sputtering of SiC films on Ni photonic crystals layers. Results show that SiC coatings have a preferential growth on the Ni skeletons, which enables them to be well bonding. The emissivity studies show that Ni PCs/SiC patterned coatings have enhanced emissive performance attributed to both the interior periodic structure and rough surfaces. The results here highlight a novel and effective structure for high emissivity coatings. It is also a new path to create highly ordered metal–ceramics composites microstructures with excellent properties and structural fidelity for thermophotovoltaic radiator, pyroelectric and other photonics applications.

Acknowledgements

We thank National Natural Science Foundation of China (Nos. 51010005, 90916020, 51174063 and 51102068), the Program for New Century Excellent Talents in University (NCET-08-0168), and the Fundamental Research Funds for the Central Universities (HIT.ICRST.2010001) and Sino-German joint project (GZ550).

References

[1] G. Neuer, G. Jaroma-Weiland, Spectral and total emissivity of high temperature materials, International Journal of Thermophysics 19 (1998) 917–929.
[2] B.V. Cockeram, D.P. Measures, A.J. Mueller, The development and testing of emissivity enhancement coatings for thermophotovoltaic (TPV) radiator applications, Thin Solid Films 355 (1999) 17–25.
[3] J. Yi, X.D. He, Y. Sun, Y. Li, Electron beam-physical vapor deposition of SiC/SiO_2 high emissivity thin film, Applied Surface Science 253 (2007) 4361–4366.
[4] K.W. Sun, W.C. Zhou, X.F. Tang, Z.B. Huang, F. Lou, D.M. Zhu, Effect of the heat treatment on the infrared emissivity of indium tin oxide (ITO) films, Applied Surface Science 257 (2011) 9639–9642.
[5] H. Tang, T.Z. Xin, Q. Sun, C.G. Yi, Z.H. Jiang, F.P. Wang, Influence of $FeSO_4$ concentration on thermal emissivity of coatings formed on titanium alloy by micro-arc oxidation, Applied Surface Science 257 (2011) 10839–10844.
[6] M.T. Ta, J.Y. Rolland, P. Echegut, B. Rousseau, M. Zaghrioui, F. Giovannelli, H. Gomart, P. Lenormand, F. Ansart, Prediction of thermal radiative properties (300–1000 K) of La_2NiO_4 ceramics, Applied Physics Letters 97 (2010) 181917.
[7] L.A. Dombrovsky, B. Rousseau, P. Echegut, J.H. Randrianalisoa, D. Baillis, High temperature infrared properties of YSZ electrolyte ceramics for SOFCs: experimental determination and theoretical modeling, Journal of the American Ceramic Society 94 (2011) 1–7.
[8] X. Zhao, X.D. He, Y. Sun, L.D. Wang, Carbon nanotubes doped SiO_2/SiO_2–PbO double layer high emissivity coating, Materials Letters 65 (2011) 2592–2594.
[9] H.Z. Liu, Z.G. Liu, J.H. Ouyang, Y.M. Wang, Thermo-optical properties of $LaMg_{1-x}Ni_xAl_{11}O_{19}$ ($0 \le x \le 1$) hexaaluminates for metallic thermal protection system, Materials Letters 65 (2011) 2614–2617.
[10] G.J. Feng, Y. Wang, Y. Li, J.T. Zhu, L. Zhao, Greatly enhanced infrared normal spectral emissivity of microstructured silicon using a femtosecond laser, Materials Letters 65 (2011) 1238–1240.
[11] J.G. Fleming, S.Y. Lin, I. El-Kady, R. Biswas, K.M. Ho, All-metallic three-dimensional photonic crystals with a large infrared bandgap, Nature 417 (2002) 52–55.
[12] V. Shklover, L. Braginsky, G. Witz, M. Mishrikey, C. Hafner, High-temperature photonic structures: thermal barrier coatings, infrared sources and other applications, Journal of Computational and Theoretical Nanoscience 5 (2008) 862–893.
[13] Y.X. Yeng, M. Ghebrebrhan, P. Bermel, W. Chan, J.D. Joannopoulos, M. Soljačić, I. Celanovic, Enabling high-temperature nanophotonics for energy applications, Proceedings of the National Academy of Sciences of the United States of America 109 (2012) 2280–2285.
[14] J.M. Zhou, H.L. Li, L. Ye, J. Liu, J.X. Wang, T. Zhao, L. Jiang, Y.L. Song, Facile fabrication of tough SiC inverse opal photonic crystals, Journal of Physical Chemistry C 114 (2010) 22303–22308.
[15] Y.G. Xu, M. Guron, X.L. Zhu, L.G. Sneddon, S. Yang, Template synthesis of 3D high-temperature silicon-oxycarbide and silicon-carbide ceramic photonic crystals from interference lithographically patterned organosilicates, Chemistry of Materials 22 (2010) 5957–5963.
[16] Y. Li, B. Ma, J.P. Zhao, W.H. Xin, X.J. Wang, Excellent mechanical properties of three dimensionally ordered macroporous nickel photonic crystals, Journal of Alloys and Compounds 509 (2011) 290–293.
[17] Y. Li, X.S. Fang, N. Koshizaki, T.i. Sasaki, L. Li, S.Y. Gao, Y. Shimizu, Y. Bando, D. Golberg, Periodic TiO_2 nanorod arrays with hexagonal nonclose-packed arrangements: excellent field emitters by parameter optimization, Advanced Functional Materials 19 (2009) 2467–2473.
[18] S. Jeong, E.C. Garnett, S. Wang, Z.F. Yu, S.H. Fan, M.L. Brongersma, M.D. McGehee, Y. Cui, Hybrid silicon nanocone–polymer solar cells, Nano Letters 12 (2012) 2971–2976.
[19] H.X. Zhang, P.X. Feng, V. Makarov, B.R. Weiner, G. Morell, Synthesis of nanostructured SiC using the pulsed laser deposition technique, Materials Research Bulletin 44 (2009) 184–188.
[20] C.Y. Luo, A. Narayanaswamy, G. Chen, J.D. Joannopoulos, Thermal radiation from photonic crystals: a direct calculation, Physical Review Letters 93 (2004) 213905.
[21] L. Zhen, Y.X. Gong, J.T. Jiang, C.Y. Xu, W.Z. Shao, P. Liu, J. Tang, Synthesis of CoFe/Al_2O_3 composite nanoparticles as the impedancematching layer of wideband multilayer absorber, Journal of Applied Physics 109 (2011) 07A332.
[22] Q.Z. Zhu, Z.M. Zhang, Correlation of angle-resolved light scattering with the microfacet orientation of rough silicon surfaces, Optical Engineering 44 (2005) 073601.